ELSEVIER

Cement & Concrete Composites 25 (2003) 31–41

Cement & Concrete Composites

www.elsevier.com/locate/cemconcomp

# Strength and strain capacities of concrete compression members reinforced with FRP

G. Campione *, N. Miraglia

*Dipartimento di Ingegneria, Strutturale e Geotecnica, Università di Palermo, Viale delle Scienze, 90128 Palermo, Italy*

Received 15 March 2001; accepted 26 April 2001

**Abstract**

The analytical compressive behavior of concrete members reinforced with fiber-reinforced polymer (FRP) was examined. The variation in the shape of the transverse cross-section was analyzed. The bearing capacity and the increase in the maximum strain for members having a cross-section which was circular, square or square with round corners reinforced with FRP were determined. The proposed analytical model allows one to evaluate the confining pressure in ultimate conditions considering the effective confined cross-section and also allows one to determine the ultimate strain corresponding to FRP failure through a simplified energetic approach. Analytical results are then compared to experimental values available in the literature, showing good agreement.


*Keywords:* Fiber-reinforced polymer; Confinement; Compressive strength; Ultimate strain

## 1. Introduction

Several theoretical and experimental investigations [1,2] are concerned with calculating the strength and ductility of compressed concrete elements with traditional confinement steel reinforcements (spirals, hoops, stirrups) and having circular or rectangular transverse cross-section. These studies have shown that the presence of transverse steel reinforcement increases the bearing capacity of compressed members due to the triaxial stress state which arises in the concrete core. In structural members confined with steel spirals the maximum increase in bearing capacity and ductility is higher with respect to that obtained utilizing circular steel hoops and with respect to that obtained in square or rectangular sections.

More recently the interest in using composite material, like fiber-reinforced polymer (FRP), for retrofitting or strengthening of concrete structures, has led to the attention of researchers and of the industry on the topic of confinement due to the presence of FRP.

It was shown [3–13] that the use of FRP materials offers almost always an increase in strength and ductility, and also several advantages with respect to traditional concrete structures, like the non-corrodibility and the lightness of composite materials, and ease of application in real structures.

Focusing the attention on the behavior of compression members, the main parameters investigated in literature [3–13] are the type of FRP material (carbon, aramid, glass, etc.) and its manufacture (unidirectional or bi-directional wraps), the shape of the transverse cross-section of the members, the dimensions and the shape of specimens, the strength of concrete, the types and percentages of steel reinforcements.

As already observed for concrete members confined with steel transverse reinforcements, also in members reinforced with FRP there is a greater increase in strength [9] for members having circular transverse cross-section, compared to those having square or rectangular transverse cross-section, the latter showing in some cases no increase in strength due to the presence of FRP.

In the present investigation an analytical model to predict maximum strength and ultimate strain of concrete confined with FRP is proposed. Compression members having different shapes of transverse cross-sections, also in the presence of longitudinal steel reinforcements

* Corresponding author. Tel.: +39-091-656-8467; fax: +39-091-656-8407.

*E-mail address:* campione@stru.diseg.unipa.it (G. Campione).

0958-9465/03/$ - see front matter 
PII: S0958-9465(01)00048-8

**Nomenclature**

| | |
|---|---|
| $A_a$ | area of longitudinal steel |
| $A_c$ | area of core of section within centerlines of FRP perimeter |
| $A_{cc}$ | area of core within centerlines of FRP perimeter excluding area of longitudinal steel |
| $A_f$ | area of FRP in the cross-section |
| $b_d$ | concrete core dimension to centerline of FRP perimeter |
| $E_f$ | modulus of elasticity of FRP |
| $E_0$ | initial concrete modulus of elasticity |
| $f'_c$ | compressive strength of unconfined concrete |
| $f'_{cc}$ | compressive strength (peak stress) of confined concrete |
| $f_y$ | yield stress of steel |
| $f_l$ | lateral confining stress on concrete core from FRP transverse reinforcement |
| $f'_l$ | effective lateral confining stress |
| $f_r$ | stress in FRP wraps |
| $f_{st}$ | stress of FRP composite |
| $f_u$ | ultimate strength of FRP |
| $N_u$ | ultimate load of FRP confined compressed section |
| $k_e$ | confinement effectiveness coefficient |
| $k_i$ | reduction factor of FRP stress due to the shape of the cross-section |
| $k_1$ | concrete strength enhancement coefficient |
| $r$ | corner radius of cross-section |
| $t$ | thickness of FRP layers |
| $U_{cc}$ | ultimate strain energy per unit volume of confined concrete |
| $U_{sl}$ | energy required to maintain yield in the longitudinal steel in compression |
| $U_{co}$ | ultimate strain energy per unit volume of unconfined concrete |
| $U_{st}$ | ultimate energy per unit volume spent to break the composite FRP |
| $\varepsilon_{co}$ | strain at maximum stress of unconfined concrete |
| $\varepsilon_{cf}$ | strain of FRP composite measured at failure on the middle of the side in the cross-section |
| $\varepsilon_{cu}$ | ultimate concrete compressive strain defined as strain at FRP failure in tension |
| $\varepsilon_f$ | ultimate strain of FRP composite |
| $\varepsilon_{su}$ | strain of FRP composite |
| $\Delta\varepsilon$ | increase in maximum strain |
| $\mu$ | increase in maximum strain of FRP-confined concrete compared to that of unconfined concrete |
| $\rho_{cc}$ | ratio of longitudinal reinforcement $A_a$ to the area of cross-section $A_c$ |
| $\rho_f$ | transverse FRP reinforcement ratio |

and confinement with FRP wraps are analyzed. Lastly, the analytical results are compared with experimental results available in the literature [4,5,7–9,13] showing the good agreement achieved with the proposed model.

## 2. Strength of compression members reinforced with FRP

As already mentioned, the use of FRP materials in concrete compression members produces an increase in strength depending on the FRP properties (material type, strength, thickness, etc.), on the concrete properties, and prevalently on the shape of the transverse cross-section.

Fig. 1 shows typical stress–strain curves of compression tests carried out by the authors [13] on concrete specimens having a cross-section which is circular or square with slightly rounded corners reinforced with FRP wraps. The wrap type is unidirectional, one layer, high strength, high modulus carbon fiber having thickness $t = 0.165$ mm, modulus of elasticity $E_f = 230$ GPa, ultimate strength $f_u = 3430$ MPa and ultimate strain $\varepsilon_f = 1.5\%$. The volumetric ratio of FRP reinforcement utilized is $\rho_f = 0.668\%$ and it is defined as the volumetric ratio of FRP in the unit volume of concrete core equal to $\rho_f = A_f/A_c$, with $A_f$ the area of the composite in the cross-section, and $A_c$ the area of the cross-section.

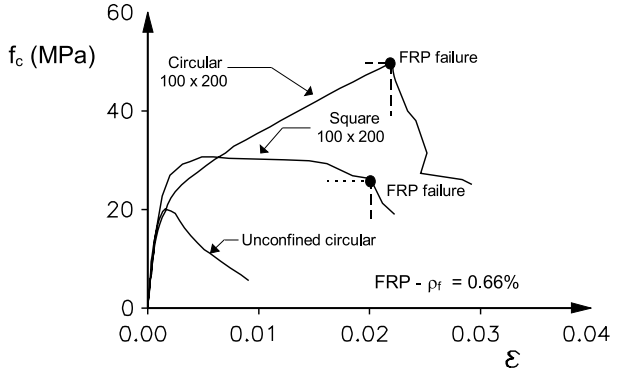


Fig. 1. Stress–strain curves for FRP-reinforced concrete specimens with different shapes of the transverse cross-section [13].

It was observed [13] that the presence of FRP reinforcement increases the strength of plain concrete, but this phenomenon is strongly influenced by the shape of the cross-section.

The effectiveness of FRP reinforcement is less in the case of a square section compared to a circular cross-section and this is due to the concentration of stresses at the corner of the square section and also to the smaller effectively confined concrete core in a square section with respect to a circular cross-section. As a consequence of this, in order to obtain in columns having a square cross-section analogous performance in terms of strength as in columns having a circular transverse cross-section and reinforced with FRP, an increase in the volumetric ratio of FRP is required and/or a transformation of the square section into one with rounded corners, utilizing adequate corners radii. To do this it is possible to modify the shape of the square section, before the application of FRP, by adding new concrete on the sides of the square section until the desired shape is obtained.

In the present investigation the effect of FRP on the confinement action in compression concrete members with variation in the shape of the transverse cross-section, shown in Fig. 2, is analyzed.

The cases of circular ($r = b_d/2$) and square ($r = 0$) sections form the limits of the square section with round corners.

In the following exposition, the attention is on the determination of the effective confinement pressure and on the determination of the effectively confined area of concrete core.

Experimental research [1] has shown that in the presence of a triaxial stress state the effective pressure determining failure of cylindrical concrete specimens is:

$$f'_{cc} = f'_c + k_1 f'_l, \tag{1}$$

$f'_c$ being the ultimate cylindrical strength of plain concrete, $f'_l$ the effective lateral pressure confining the concrete core due to FRP and $k_1$ an experimental coefficient generally assumed for concrete [1] between 2.8 and 4.1.

The applicability of $k_1$ coefficient between 2.8 and 4.1 for FRP reinforcement is limited [11] due to the inherent anisotropy in the composite materials. This would result in generally poor comparison between experimental and predict results especially as related to strain [11]. In the present study, using a regression analysis of the experimental data with a correlation factor of 88%, $k_1$ equal to 2 was assumed for concrete members reinforced with FRP wraps.

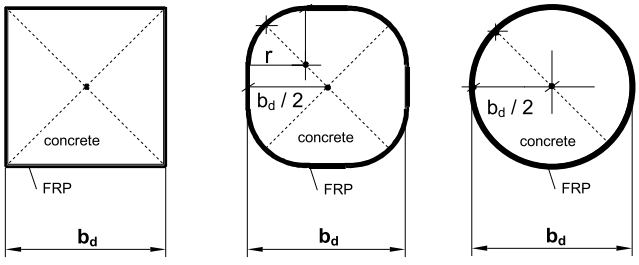


Fig. 2. Shapes of the cross-sections examined.

The increase in strength due to the effective lateral pressure $f'_l$ depends on the lateral pressure $f_l$ assumed to be uniformly distributed over the surface of the concrete core and also depends on the effectiveness coefficient $k_e$, according to the following:

$$f'_l = k_e f_l, \tag{2}$$

where

$$k_e = A_e/A_{cc} \tag{3}$$

with $A_e$ the area of the effectively confined concrete core and $A_{cc}$ the transverse area of concrete enclosed by the centerlines of the perimeter FRP defined as:

$$A_{cc} = A_c(1 - \rho_{cc}), \tag{4}$$

$\rho_{cc}$ being the ratio of longitudinal reinforcement $A_a$ to the area of cross-section $A_c$.

It is shown in the following exposition that both the coefficient $k_e$ and the pressure $f_l$ depend on the shape of the cross-section of the compression members.

### 2.1. Determination of the effective lateral confining pressure

To determine the effective confinement pressure it is possible to refer to the rigid body equilibrium of the transverse cross-section (Fig. 3) subjected to the distributed pressure $f_l$ and to the localized forces in the FRP in the ultimate condition.

The fundamental hypotheses assumed are:

- all transverse cross-sections of the members are in the same condition along the height of the members due to the presence of continuous FRP reinforcement;
- FRP behaves elastically up to failure and sudden failure occurs after the maximum strength is reached;
- perfect adhesion between concrete and FRP is ensured up to the failure of compression members.

It is important to observe that failure in tension of FRP wraps does not always occur; and the rupture of FRP occurs only when the compressive stress and the confining pressure, that are variable with the strain values, reach their maximum [11].

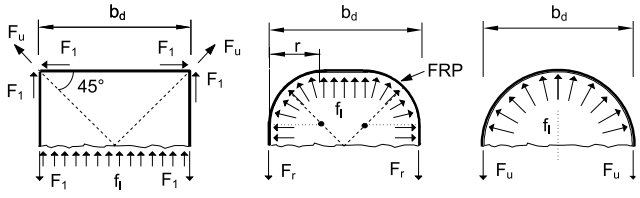


Fig. 3. Effective lateral confining pressure for FRP-reinforced cross-sections.

The analytical method here developed considers only the cases in which failure of FRP in tension occurs and further studies will be developed to extend the method to the cases in which FRP do not fail in tension.

In the case of a circular cross-section the stress in the fiber can be assumed to be uniform all along the perimeter of the circumference; instead, in a square cross-section the stress is not uniform along the perimeter because of stress concentration near the corners of the section. In an approximate way this can be taken into account by considering a constant reduced uniform stress all along the perimeter equal to $f_r$, as shown in the following paragraph.

Because of the equilibrium of the forces in the FRP at the corners of the cross-section the maximum action acting in the direction parallel to the sides of the section is $0.707F_u = 0.707tf_u$. The coefficient 0.707 is obtained by considering that the resulting forces at the corners of the square section have the direction of the diagonal of the square section and because of the equilibrium of the forces the maximum value $F_u$ allowed in the direction parallel to the sides of the square section is $F_l = 0.707F_u$.

In the case of a square section with round corners the presence of round-filled corners reduces the concentration of stresses at the corners, ensuring a more gradual variation in stress, with values between those related to the cases of circular and square cross-sections.

By considering, in a simplified way, the stress $f_r$ in FRP variable with the radii of the corners $r$ it is possible to obtain:

$$f_r = f_u \left[ \left( 1 - \frac{\sqrt{2}}{2} k_i \right) \frac{2r}{b_d} + k_i \frac{\sqrt{2}}{2} \right], \tag{5}$$

$k_i$ being a reduction factor of the stress determined experimentally and introduced in (5) to take into account the stress intensification in FRP at the corners. As it will be shown in the section relative to the comparison with the experimental data, assuming a constant value of $k_i$ equal to 0.2121, a best fitting of experimental data was obtained with a correlation factor of 92%.

By considering the equilibrium of forces in the transverse cross-section shown in Fig. 3 subjected to internal confining pressure $f_l$ and to the concentrated forces at the free end of the FRP, it is possible to obtain the expressions of $f_l$ for the cases examined.

For a cross-section which is circular, square with round corners or square we obtained:

$$f_l = \frac{2tf_u}{b_d} \quad \text{circular}, \tag{6}$$

$$f_l = \frac{2tf_r}{b_d} \quad \text{square with round corners}, \tag{7}$$

$$f_l = \frac{\sqrt{2}tf_u}{b_d} k_i \quad \text{square}. \tag{8}$$

### 2.2. Effectiveness coefficient $k_e$

For the determination of the effectiveness factor $k_e$ it can be assumed (see Fig. 4) that, in the case of a circular cross-section, the entire concrete core internal to the perimeter of FRP is effectively confined, while, for the square section there is a reduction in the effectively confined core that can be assumed, analogously with the case of concrete core confined by transverse steel stirrups [1], in the form of a second-degree parabola with an initial tangent slope of 45°.

For the square section with round corners it can be assumed, as also suggested by experimental observation [13], that the presence of round corners produces at the corners a further effective confinement area with respect to the case of the square section, leading to a more effective confined core represented by the area enclosed by the parabola and by the round corners, as shown in Fig. 4. The effectively confined concrete core shown in Fig. 4 is represented with the hatched area.

Based on this observation, it is possible to obtain the $k_e$ factor that, for a square section with round corners, is:

$$k_e = \frac{\left[ b_d^2 - 4\left( r^2 - \frac{\pi r^2}{4} \right) \right] - \frac{2}{3}(b_d - 2r)^2}{b_d^2 - 4\left( r^2 - \frac{\pi r^2}{4} \right)}. \tag{9}$$

This factor assumes values of $k_e = 1$ for a circular section and of $k_e = 1/3$ for a square section. The latter is in accordance with the hypothesis that the reduction in the volume of effectively confined concrete is due only to the reduction of effectively confined area of the transverse cross-section.

Fig. 5 shows the variation in $k_e$ with $r/b_d$. It is interesting to observe that, for values of $r/d_b$ above 0.2, 80% of the total transverse area of the cross-section is effectively confined.

Having determined the effective lateral pressure $f_l'$, it is possible to evaluate the strength $N_u$ of a compressed member confined with FRP, also in the pres-

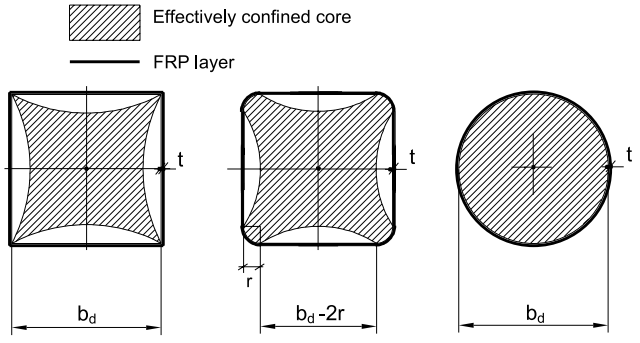


Fig. 4. Effective confined concrete core of cross-section reinforced with FRP.

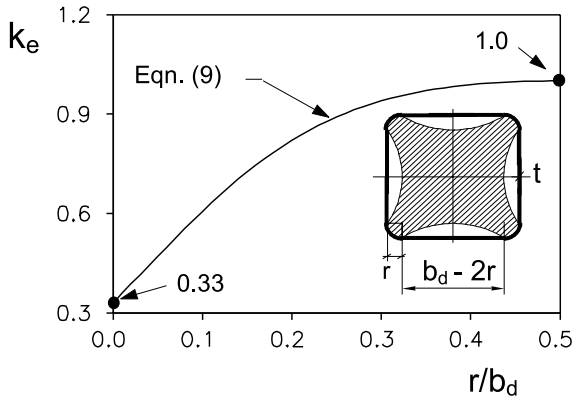


Fig. 5. Variation in the effectiveness coefficient $k_e$ with $r/b_d$.

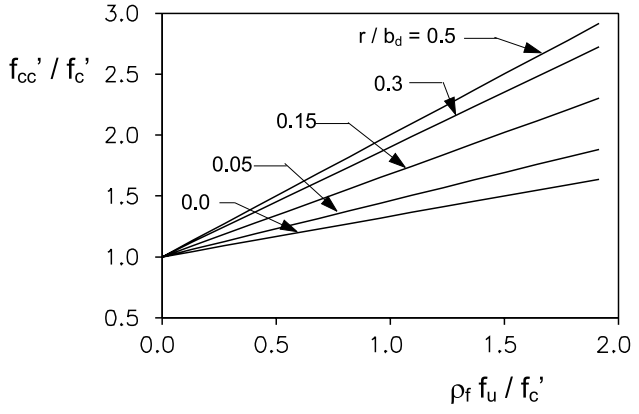


Fig. 6. Increase in the compressive strength with $\rho_f f_u/f'_c$.

ence of longitudinal steel reinforcements, utilizing the superposition principle and separately considering the contribution due to the presence of FRP evaluated by using (1) and the contribution due to the longitudinal steel of area $A_a$ assumed to have yielded, as follows:

$$N_u = f'_c A_c + f_y A_a + k_1 k_e f_l A_c. \tag{10}$$

Fig. 6, for some values of the parameter $r/b_d$, shows the variation in maximum strength $f'_{cc}$ referred to that of unconfined plain concrete $f'_c$ with the parameter $\rho_f f_u/f'_c$ for the different section types examined. It is interesting to observe that, to get a prefixed strength value, the amount of volume percentages of FRP greatly depends on the shape of the section. In particular a square section reinforced with FRP having the same strength as a circular section requires higher percentages of FRP, which is not cheap at present.

## 3. Monotonical stress–strain relationship for compressed members confined with FRP

For the analytical modeling of the complete compressive stress–strain curves of FRP-confined members

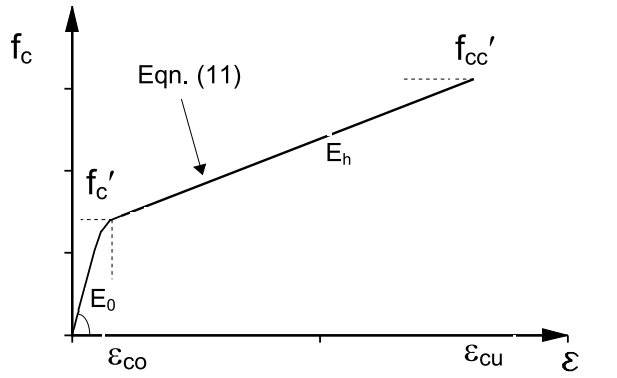


Fig. 7. Stress–strain model in compression for FRP confined concrete members.

the following relationship, which is also represented in Fig. 7, can be utilized:

$$\frac{f_c}{f'_c} = \beta \frac{\varepsilon}{\varepsilon_{co}} + \left\{ \left\{ (1-\beta) \frac{\varepsilon}{\varepsilon_{co}} \right\} \Big/ \left\{ \left[ 1 + \left( \frac{\varepsilon}{\varepsilon_{co}} \right)^R \right]^{1/R} \right\} \right\}, \tag{11}$$

where

$$\beta = \frac{E_h}{E_0}; \qquad E_h = \frac{f'_{cc} - f'_c}{\varepsilon_{cu} - \varepsilon_{co}}. \tag{12}$$

This model is a revised version of the well-known Pinto and Giuffrè [14] model originally proposed for stress–strain curves of steel. The (11) relationship represents a curved transition from a straight line asymptote with slope $E_0$, $E_0$ being the initial modulus of FRP concrete, to another asymptote with slope $E_h$. The $\beta$ parameter is the strain hardening ratio, that is the ratio between slope $E_h$ and $E_0$ and $R$ is a parameter which influences the shape of the transition curve and here assumed constant and equal to 3 to reproduce with good approximation experimental results.

The hardening part is governed by the strength and by the maximum strain characteristics of confined and unconfined concrete. The stress–strain curve stops when the maximum stress $f'_{cc}$ and maximum strain $\varepsilon_{cu}$ are reached and FRP breaks in tension because its ultimate strain has been reached. The proposed equation for stress–strain curve (11), as it will shown in the following section relative to comparison which experimental data, fits very well the experimental data referring to the cases in with FRP produces strain-hardening in concrete specimens (i.e. for the case of cylindrical specimens), instead in the cases in which the increase of strength due to the presence of FRP is negligible (i.e. cases of square section), no good prediction is expected.

## 4. Ultimate concrete strain at FRP failure

To determine the ultimate axial strain of confined concrete core $\varepsilon_{cu}$ the well-known model proposed by Mander et al. [1] based on the energy balance approach was considered, though we also consider the contribution due to the presence of FRP.

The energy balance equation can be written as follows:

$$U_{st} = U_{cc} - U_{co} + U_{sl}, \tag{13}$$

where $U_{st}$ is the ultimate strain energy per unit volume spent to break the composite FRP:

$$U_{st} = \rho_f A_c \int_0^{\varepsilon_{us}} f_{st}\, d\varepsilon_{st}. \tag{14}$$

$U_{cc}$ is the ultimate strain energy per unit volume of confined concrete:

$$U_{cc} = A_c \int_0^{\varepsilon_{cu}} f_c\, d\varepsilon_c. \tag{15}$$

$U_{co}$ is the ultimate strain energy per unit volume of unconfined concrete:

$$U_{co} = A_c \int_0^{2\varepsilon_0} f_{uc}\, d\varepsilon_c. \tag{16}$$

$U_{sl}$ is the energy per unit volume required to maintain yield in the longitudinal steel in compression:

$$U_{sl} = \rho_{cc} A_c \int_0^{\varepsilon_{cu}} f_{sl}\, d\varepsilon_{sl}. \tag{17}$$

$\varepsilon_{us}$ being the ultimate strain of the composite, $f_{st}$ and $\varepsilon_{st}$ the stress and the strain in the composite.

By substituting the expressions (14)–(17) into (13) it is possible, knowing the complete stress–strain relationship of materials, to obtain the ultimate strain of concrete core $\varepsilon_{cu}$.

In an approximate way it is possible to obtain the ultimate strain of the concrete core $\varepsilon_{cu}$ knowing only the maximum strength of the unconfined and confined concrete core. As shown in Fig. 8, in the cases of both plain concrete and FRP confined concrete, the area subtended under the stress–strain curves represents the energy per unit volume spent to break the concrete in compression and corresponding to the strain values determining FRP failure in tension. If the contribution due to the longitudinal steel to maintain yield is neglected, to simplify the calculation, the difference between the area subtended by the stress–strain curve of confined concrete less the area subtended under the stress–strain curves of the unconfined concrete represents the energy spent to produce failure of FRP.

In this case the ultimate strain $\varepsilon_{cu}$ can be obtained by the following:

$$\varepsilon_{cu} = \varepsilon_{co} + \Delta\varepsilon. \tag{18}$$

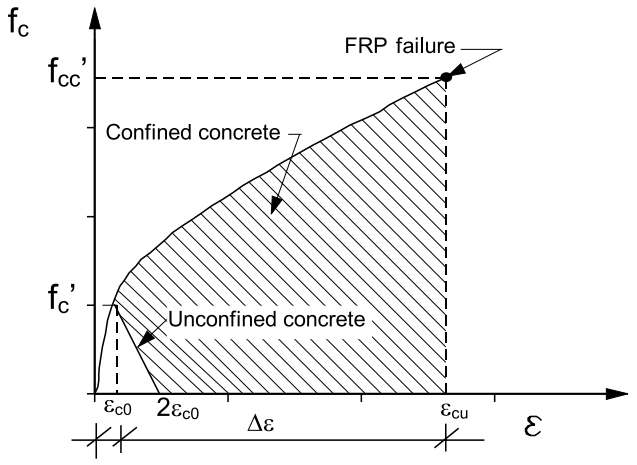


Fig. 8. Stress–strain model in compression for calculation of ultimate concrete strain.

By setting the area subtended under the $f_c$–$\varepsilon$ diagram in compression (Fig. 8) equal to the internal work performed to break the FRP in tension through the cross-section of the confined concrete core, it is possible to obtain the increase in strain $\Delta\varepsilon$ and hence the maximum strain $\varepsilon_{cu}$. The energy per unit volume of confined concrete can be calculated approximately as the area of the trapezium having sides $f'_{cc}$ and $f'_c$ and base $\Delta\varepsilon$.

This approximation is validated by the following considerations: the shape of the effective stress–strain curve $f_c$–$\varepsilon$ due to the presence of FRP is approximately linear after $f'_c$ is reached; the area subtended up to the $f'_c$ of the unconfined concrete is negligible compared to the other quantities.

The energy spent to break the FRP wraps, having area of the transverse cross-section $A_f$, can be evaluated exactly by using (13) and setting the two above-mentioned areas equal as follows:

$$\frac{1}{2}\Delta\varepsilon\left(f'_{cc} + f'_c\right)A_c = A_f \frac{1}{E_f} f_r^2, \tag{19}$$

which gives the increase in maximum strain $\Delta\varepsilon$:

$$\Delta\varepsilon = 2\rho_f \frac{f_r^2}{E_f} \frac{1}{2f'_c + k_1 k_e f_l} \quad \text{with}$$
$$\rho_f = \frac{2\left[2\left(b_d - 2r\right) + \pi r\right]t}{b_d^2 - 4\left(r^2 - \left(\pi r^2/4\right)\right)} \tag{20}$$

or in extended form

$$\Delta\varepsilon = \frac{2f_r^2}{E_f} \frac{\left[2\left(b_d - 2r\right) + \pi r\right]t}{b_d^2 - 4\left(r^2 - \left(\pi r^2/4\right)\right)} \left\{ 1 \Big/ \left\{ f'_c + k_1 \frac{t}{b_d} f_r \times \frac{\left[b_d^2 - 4\left(r^2 - \frac{\pi r^2}{4}\right)\right] - \frac{2}{3}\left(b_d - 2r\right)^2}{b_d^2 - 4\left(r^2 - \frac{\pi r^2}{4}\right)} \right\} \right\}. \tag{21}$$

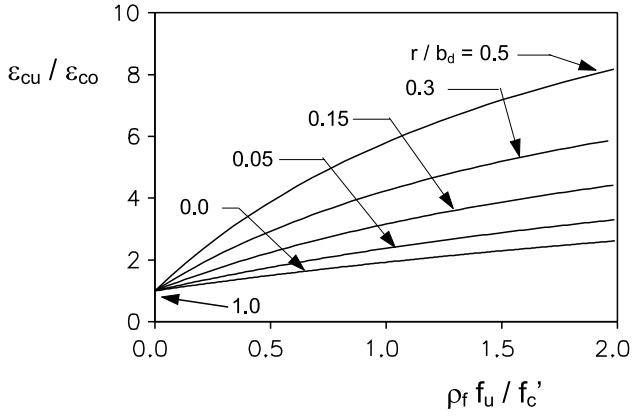


Fig. 9. Increase in the ultimate strain with $\rho_f f_u/f'_c$.

Assuming $k_1 = 2$, as already mentioned in accordance with experimental data, the increase, $\mu = (\varepsilon_{co} + \varepsilon)/\varepsilon_{co}$, in maximum strain of FRP confined concrete compared to that of unconfined concrete is

$$\mu = 1 + \rho_f \frac{1}{\varepsilon_{co}} \frac{f_r^2}{E_f} \frac{1}{f'_c + k_e f_l}. \quad (22)$$

Fig. 9 shows the variation in the parameter $\varepsilon_{cu}/\varepsilon_{co}$ with $\rho_f f_u/f'_c$ for the different cases examined, highlighting the importance of the shape of the cross-section in the ultimate deformation capacity in compression of a concrete core confined by FRP.

## 5. Comparison between analytical and experimental results

In the present section some experimental results on the use of FRP materials for confining concrete, recently presented in the literature [3–13], are presented for comparison with analytical results.

The above-mentioned results regard compressive tests on prismatic and cylindrical specimens of different sizes, reinforced with different types of FRP materials (carbon, glass, aramid, etc.), with different concrete strengths. Tests on prismatic specimens regard members reinforced with carbon fiber and having a square cross-section with rounded corners with different radii $r$ of the corner ($r = 3, 5, 25$ and 38 mm). In all tests, unidirectional fiber wraps with an anchorage length (generally between 50 and 100 mm) necessary to avoid sliding or debonding of fibers during the tests were utilized and rupture of fibers was always observed.

Table 1 gives average values for the cases mentioned [4,5,7–9,13]: dimensions and shapes of the specimens

Table 1
Characteristics of specimens and materials tested

| Code | Refs. | Concrete type | | | | Mater. | FRP characteristics | | | | |
|---|---|---|---|---|---|---|---|---|---|---|---|
| | | $b_d$ (mm) | $r$ (mm) | $f'_c$ (MPa) | $\varepsilon_{co}$ (%) | | $t$ (mm) | $\rho_f$ (%) | $E_f$ (GPa) | $\varepsilon_f$ (%) | $f_u$ (MPa) |
| C1 | [13] | 100 | 0 | 20.05 | 0.207 | Carbon | 0.165 | 0.66 | 230 | 1.5 | 3430 |
| SR1 | [13] | 100 | 3 | 20.05 | 0.207 | Carbon | 0.165 | 0.66 | 230 | 1.5 | 3430 |
| C2 | [3] | 150 | 0 | 36.90 | 0.250 | Carbon | 0.167 | 0.44 | 235 | 1.5 | 3510 |
| C3 | [3] | 150 | 0 | 36.90 | 0.250 | Carbon | 0.501 | 1.34 | 235 | 1.5 | 3510 |
| C4 | [3] | 150 | 0 | 36.90 | 0.250 | Glass | 1.20 | 3.20 | 26 | 1.6 | 399 |
| C5 | [3] | 150 | 0 | 36.90 | 0.250 | Glass | 3.60 | 9.60 | 26 | 1.6 | 399 |
| C6 | [7] | 190.6 | 0 | 27.07 | 0.198 | Carbon | 0.22 | 0.46 | 230 | 1.5 | 3483 |
| C7 | [7] | 190.6 | 0 | 27.07 | 0.198 | Carbon | 0.22 | 0.46 | 230 | 1.5 | 3483 |
| C8 | [5] | 155 | 0 | 60.00[a] | / | Carbon | 0.13 | 0.33 | 230 | 1.5 | 3500 |
| C9 | [5] | 155 | 0 | 60.00[a] | / | Carbon | 0.26 | 0.67 | 230 | 1.5 | 3500 |
| C10 | [5] | 155 | 0 | 60.00[a] | / | Carbon | 0.39 | 1.00 | 230 | 1.5 | 3500 |
| C11 | [9] | 100 | 0 | 42.00 | / | Carbon | 0.60 | 2.41 | 82.70 | 1.5 | 1265 |
| C12 | [9] | 150 | 0 | 43.00 | / | Aramid | 1.26 | 3.93 | 13.60 | 1.69 | 230 |
| C13 | [9] | 150 | 0 | 43.00 | / | Aramid | 2.52 | 6.83 | 13.60 | 1.69 | 230 |
| C14 | [9] | 150 | 0 | 43.00 | / | Aramid | 3.78 | 10.30 | 13.60 | 1.69 | 230 |
| C15 | [9] | 150 | 0 | 43.00 | / | Aramid | 5.04 | 13.90 | 13.60 | 1.69 | 230 |
| SR2 | [9] | 152 | 5 | 43.90 | / | Carbon | 1.50 | 3.93 | 82.70 | 1.5 | 1265 |
| SR3 | [9] | 152 | 25 | 43.90 | / | Carbon | 1.50 | 3.79 | 82.70 | 1.5 | 1265 |
| SR4 | [9] | 152 | 38 | 35.80 | / | Carbon | 1.50 | 3.76 | 82.70 | 1.5 | 1265 |
| SR5 | [9] | 152 | 38 | 42.00 | / | Carbon | 1.50 | 2.25 | 82.70 | 1.5 | 1265 |
| C16 | [8] | 300 | 0 | 32.00 | 0.250 | Carbon | 0.30 | 0.40 | 84.00 | 1.5 | 1770 |
| C17 | [8] | 300 | 0 | 44.00 | 0.270 | Carbon | 0.30 | 0.40 | 84.00 | 1.5 | 1770 |
| C18 | [8] | 300 | 0 | 44.00 | 0.270 | Carbon | 0.90 | 1.20 | 84.00 | 1.5 | 1770 |
| S1 | [8] | 300 | 0 | 32.00 | 0.250 | Carbon | 0.90 | 1.20 | 84.00 | 1.5 | 1770 |

C = circular; S = square; SR = square with circular corners.
[a] Determined on cube 150 × 150 mm².

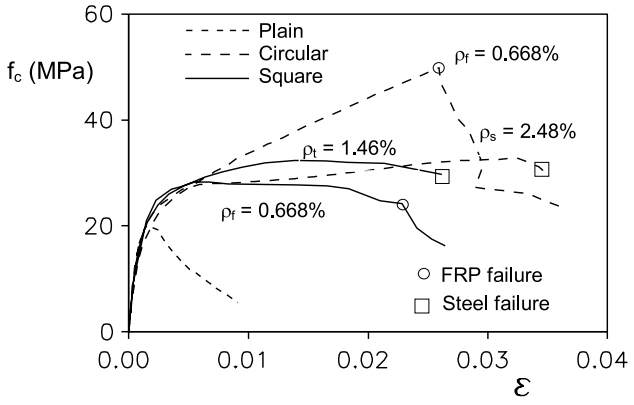


Fig. 10. Stress–strain curves for $100 \times 200$ mm$^2$ concrete specimens confined with CFRP and/or transverse steel reinforcements.

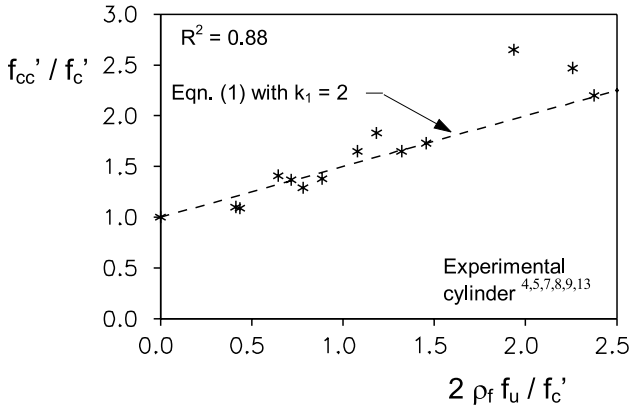


Fig. 13. Variation in compressive strength with $2\rho_f f_u/f'_c$.

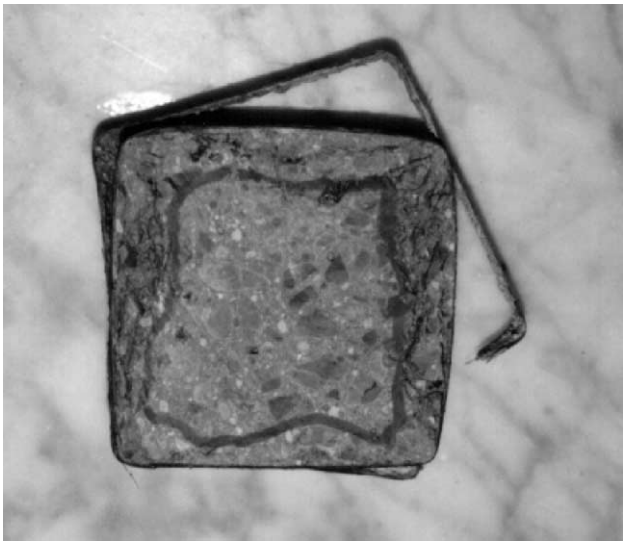

Fig. 11. Transverse cross-section of compressed concrete members with square section confined with FRP at failure [13].

tested; mechanical characteristics and volumetric percentages of fibers utilized; mechanical properties of unconfined concrete.

Of particular interest is the experimental investigation of Rochette [9] in which the influence of the shape of the cross-section and the types and volumetric percentage of fibers on the compressive behavior of concrete members reinforced with FRP was examined. In the same investigation the strain in FRP was also recorded during the tests, and based on these results it was possible to calibrate the $k_i$ factor.

It emerges from all the mentioned experimental investigations that the use of FRP produces a significant change in the behavior of plain concrete in terms of both maximum strength and strain. In particular, a significant increase in maximum strength was observed for the circular cross-section; instead less effective confinement was observed for square sections or square sections with round corners. This is due to the intensification of stresses at the corners and consequently to the lower confining pressure and smaller effective concrete core

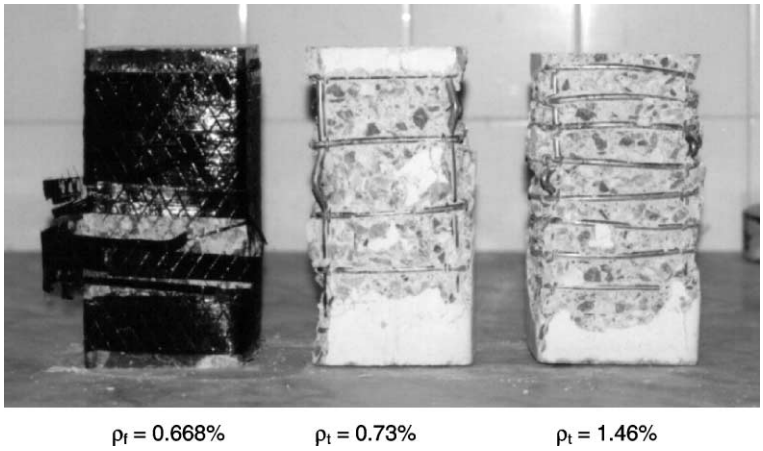


Fig. 12. Mode of failure of concrete specimens reinforced with transverse steel reinforcement and FRP [13].

Table 2
Mechanical properties of tested specimens

| Code | Experimental values | | | | Analytical values | | | |
|---|---|---|---|---|---|---|---|---|
| | $f'_{cc}$ (MPa) | $f'_{cc}/f'_c$ | $\varepsilon_{cu}$ (%) | $\varepsilon_{cf}$ (%) | $f'_{cc}$ (MPa) (1) | $f'_{cc}/f'_c$ | $\varepsilon_{cu}$ (%) (21) | $\varepsilon_{cf}$ (%) |
| C1 | 49.60 | 2.47 | 2.55 | / | 42.69 | 2.13 | 1.07 | / |
| SR1 | 31.15 | 1.55 | 2.25 | / | 21.91 | 1.09 | 0.64 | 0.29 |
| C2 | 47.60 | 1.29 | 0.80 | / | 52.53 | 1.42 | 0.77 | / |
| C3 | 81.10 | 2.20 | 1.40 | / | 83.79 | 2.27 | 1.41 | / |
| C4 | 52.30 | 1.41 | 1.80 | / | 49.67 | 1.34 | 0.70 | / |
| C5 | 98.00 | 2.65 | 3.20 | / | 75.20 | 2.04 | 1.30 | / |
| C6 | 53.89 | 1.99 | 0.57 | / | 43.15 | 1.59 | 0.94 | / |
| C7 | 49.62 | 1.83 | 0.49 | / | 43.15 | 1.59 | 0.94 | / |
| C8 | 54.27 | 1.09 | 0.77 | / | 61.54 | 1.23 | 0.57 | / |
| C9 | 68.76 | 1.38 | 1.47 | / | 73.28 | 1.47 | 0.83 | / |
| C10 | 82.27 | 1.65 | 1.75 | / | 85.03 | 1.71 | 1.04 | / |
| C11 | 73.50 | 1.75 | 1.60 | / | 72.36 | 1.73 | 1.06 | / |
| C12 | 47.30 | 1.10 | 1.11 | / | 50.73 | 1.18 | 0.53 | / |
| C13 | 58.91 | 1.37 | 1.47 | 1.53 | 58.45 | 1.36 | 0.76 | 1.50 |
| C14 | 70.95 | 1.65 | 1.69 | / | 66.18 | 1.54 | 0.96 | / |
| C15 | 74.39 | 1.73 | 1.74 | / | 73.91 | 1.72 | 1.14 | / |
| SR2 | 43.90 | 1.00 | 1.02 | 0.44 | 47.29 | 1.09 | 0.32 | 0.33 |
| SR3 | 47.85 | 1.09 | 0.90 | 0.51 | 57.85 | 1.34 | 0.51 | 0.65 |
| SR4 | 68.73 | 1.92 | 2.39 | 0.86 | 66.65 | 1.55 | 0.68 | 0.87 |
| SR5 | 47.46 | 1.13 | 1.08 | / | 45.32 | 1.08 | 0.77 | / |
| C16 | 40.00 | 1.25 | 0.66 | / | 39.08 | 1.22 | 0.56 | / |
| C17 | 48.00 | 1.09 | 0.97 | / | 51.08 | 1.16 | 0.56 | / |
| C18 | 75.00 | 1.70 | 1.82 | / | 66.24 | 1.50 | 1.06 | / |
| S1 | 35.00 | 1.09 | 1.00 | / | 33.06 | 1.03 | 0.58 | / |

C = circular; S = square; SR = square with circular corners.

area. These aspects are also confirmed by experimental research carried out by Campione et al. [13].

In this connection, Fig. 10 shows typical stress–strain curves for concrete specimens with circular sections or square sections with round corners tested in compression.

For a comparison the same figure shows results related to concrete specimens confined with traditional steel reinforcement constituted by spirals or stirrups with volume percentage $\rho_s$ for spirals and $\rho_t$ for stirrups. The objective of this comparison was to show, for the same concrete bath, the confinement effects of FRP in terms of both maximum stress and strain capacities with respect to those obtained utilizing traditional transverse steel reinforcement, that is very often difficult to place in cast due to the high percentages required in critical regions.

Figs. 11 and 12 show the condition of prismatic specimens tested by Campione et al. [13] after failure occurs. Fig. 11 is related to the transverse cross-section and shows the effective concrete core and FRP failure at the corner, Fig. 12 shows the full specimens and compares the effect of the confinement due to traditional steel reinforcements with that produced by FRP. The presence of FRP, up to its failure in tension, also avoids the cover expulsion, like instead does not occur if traditional transverse steel reinforcement is utilized.

Fig. 13 shows the variation in the increase in maximum strength with $2\rho_f f_u/f'_c$ for members having a circular cross-section. The experimental data [4–13] are almost all mentioned in Fig. 13; in Table 1 are given only average values.

The results confirm that the variation in strength can be assumed linearly variable with the effective lateral pressure. In particular, for cylindrical specimens utilizing, in (1) $k_1 = 2$, a correlation factor $R^2$ of 88% was obtained. In the regression analysis utilized, to obtain

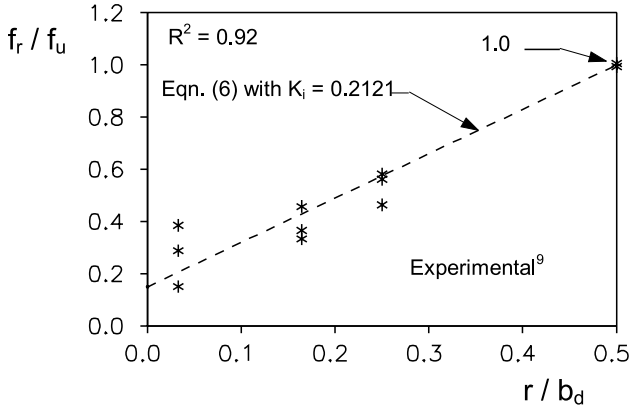


Fig. 14. Variation in effective stress in FRP with $r/b_d$.

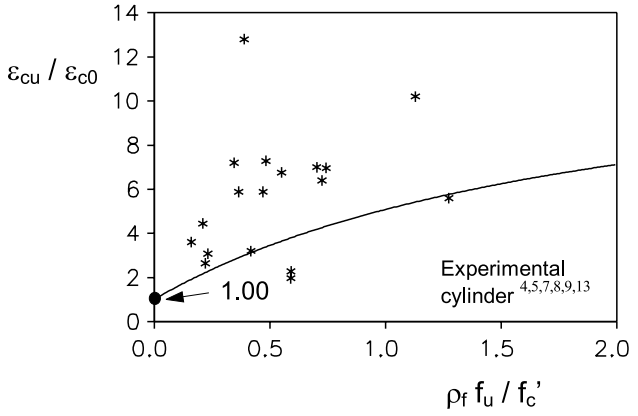


Fig. 15. Variation in ultimate strain of concrete core with $\rho_f f_u/f'_c$.

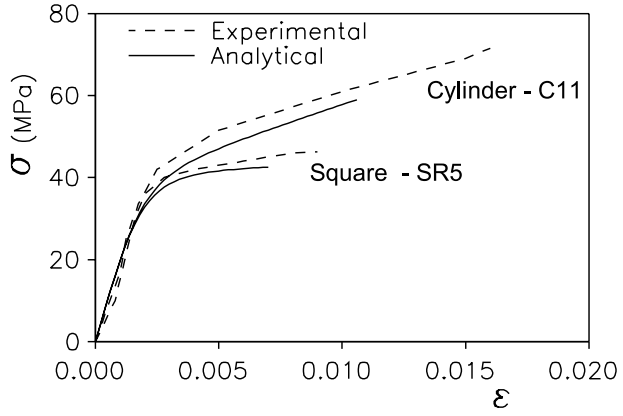


Fig. 16. Experimental and analytical comparison of stress–strain curves in compression according to data of Rochette et al. [9].

$k_1 = 2$ it was also assumed that the intercept of the straight line $f'_{cc}/f'_c$ is equal to one if $2\rho_f f_u/f'_c$ is equal to zero. In the case of specimens having transverse cross-section square and square with round corners same coefficient $k_1 = 2$ can also be assumed and good agreement with experimental data is obtained, like shown in Table 2.

Fig. 14 shows the variation in the $f_r$ stress in FRP with the variation in $r/b_d$ obtained using (5) and compared with the experimental values mentioned in Rochette et al. [9]. In this case too the assumption of a linear variation of $f_r$ with $r/b_d$ can be considered reasonable and the $k_i$ parameter can be assumed to be constant and equal to 0.2121. This coefficient calibrated on the basis of the total number of specimens examined in the literature [9] was obtained utilizing a regression analysis with $R^2 = 92\%$ and considering that the intercept of the straight line $f_r/f_u$ is equal to one if $r/b_d$ is equal to 1/2.

Fig. 15 shows the variation in maximum strain $\varepsilon_{cu}$, obtained by using (18) for the cases of members having a circular cross-section, with the parameter $\rho_f f_u/f'_c$. The figure reproduces almost all cases given in the mentioned literature [4,5,7–9,13]; instead, only average values are given in Table 2.

The results show that the analytical model to derive $\varepsilon_{cu}$ is very conservative; this can be justified by considering that the model is derived in a simplified and conservative hypothesis. As mentioned before, the strain values obtained are very conservative, but it can be accepted by considering that the experimental data utilized for comparison are related to small size specimens and if also size effects smaller ultimate strain values are expected. Table 2, as already mentioned, gives the theoretical and experimental results related to the cases mentioned in Table 1. Comparison between experimental and analytical values shows good agreement.

Fig. 16 compares the experimental stress–strain curve recorded in compression by Rochette et al. [9] with that obtained using (11). In particular results relative to specimens having circular (specimen C11) and square section with round corners with $r = 38$ mm (specimen SR5) were mentioned showing good agreement for both cases and stressing that the proposed model allows one to predict accurately the experimental response.

## 6. Conclusions

An analytical model to predict the maximum strength and the maximum strain of concrete compressed members reinforced with FRP has been presented. The influence of the shape of the transverse cross-section (circular, square and square with round corners) on the compressive behavior of members is examined.

The model allows one to obtain:

- the strength of the compressed members referring to the effective confined core depending on the shape of the cross-section;
- the reduced confining pressure in a square section with circular corners due to the concentration of stresses at the corners.

The proposed model also allows one to evaluate ultimate strain in the concrete core based on a simplified energetic approach for whose application only the geometrical and mechanical characteristics of FRP and the maximum strengths of unconfined and confined concrete are required.

The complete stress–strain relationship proposed for FRP confined concrete permits one to accurately reproduce the behavior of concrete members reinforced with FRP in agreement with the available experimental data.

Finally, further studies are required to validate the proposed equations if size effects have to be taken into

account and if failure of concrete specimens also occurs when FRP does not fail in tension.

## References


[1] Mander JB, Priestley MJN, Park R. Theoretical stress–strain model for confined concrete. ASCE J Struct Eng 1988; 114(8):1804–26.

[2] Cusson D, Paultre P. Stress–strain model for confined high strength concrete. ASCE J Struct Eng 1995;121(3):468–77.

[3] Arduini M, Di Tommaso A, Manfroni O, Ferrari S, Romagnolo M. Il confinamento passivo di elementi compressi in calcestruzzo con fogli di materiale composito. Industria Italiana del Cemento 1999;11:836–41 (in Italian).

[4] Arduini M, Di Tommaso A, Mantegazza G. Compositi per la riabilitazione strutturale. Atti delle Giornate AICAP 97 1997;1:29–240 (in Italian).

[5] Bortolotti L, Lai S, Carta S, Cireddu D. Comportamento a carico assiale di conglomerati ad alta resistenza confinati con tessuto di fibra di carbonio. Atti delle Giornate AICAP 99 1999;1:5–14 (in Italian).

[6] Mirmiran A, Shahawy M. Behavior of concrete columns confined by fiber composites. ASCE J Struct Eng 1997;123(5):583–90.

[7] Purba BK, Mufti AA. Investigation of the behaviour of circular concrete columns reinforced with carbon fiber-reinforced polymer (CFRP) jackets. Can J Civ Eng 1999;26:590–6.

[8] Demers M, Neale WK. Confinement of reinforced concrete columns with fibre-reinforced composite sheets – an experimental study. Can J Civ Eng 1999;26:26–241.

[9] Rochette P, Labossiére P. Axial testing of rectangular column models confined with composites. ASCE J Comp Construct 2000;4(3):129–36.

[10] Saadatmanesh H, Ehsani MR, Li MW. Strength and ductility of concrete columns externally reinforced with fiber composite straps. ACI Struct J 1994;91(4):434–47.

[11] Saafi M, Toutanji HA, Li Z. Behavior of concrete columns confined with fiber reinforced polymer tubes. ACI Mater J 1999;96(4):500–9.

[12] Seible F, Priesley MJN, Hegemier GA, Innamorato D. Seismic retrofit of R.C. columns with continuous carbon fiber jackets. ASCE J Compos Construct 1997;1(2):52–62.

[13] Campione G, Miraglia N, Scibilia N. Comportamento in compressione di elementi in calcestruzzo armato a sezione quadrata e circolare rinforzati con FRP. Ingegneria Sismica 2001;2 (in Italian).

[14] Pinto PE, Giuffrè A. Comportamento del cemento armato per sollecitazioni cicliche di forte intensità. Giornale del Genio Civile 1970;5 (in Italian).